The Journal of Immunology

RESEARCH ARTICLE | MARCH 15 2016

Low-Affinity Memory CD8+ T Cells Mediate Robust Heterologous Immunity

Scott M. Krummey; ... et. al

J Immunol (2016) 196 (6): 2838–2846.
https://doi.org/10.4049/jimmunol.1500639

Low-Affinity Memory CD8$^+$ T Cells Mediate Robust Heterologous Immunity

Scott M. Krummey,* Ryan J. Martinez,†,[1] Rakieb Andargachew,†,[1] Danya Liu,* Maylene Wagener,* Jacob E. Kohlmeier,† Brian D. Evavold,† Christian P. Larsen,* and Mandy L. Ford*

Heterologous immunity is recognized as a significant barrier to transplant tolerance. Whereas it has been established that pathogen-elicited memory T cells can have high or low affinity for cross-reactive allogeneic peptide–MHC, the role of TCR affinity during heterologous immunity has not been explored. We established a model with which to investigate the impact of TCR-priming affinity on memory T cell populations following a graft rechallenge. In contrast to high-affinity priming, low-affinity priming elicited fully differentiated memory T cells with a CD45RB^{hi} status. High CD45RB status enabled robust secondary responses in vivo, as demonstrated by faster graft rejection kinetics and greater proliferative responses. CD45RB blockade prolonged graft survival in low affinity–primed mice, but not in high affinity–primed mice. Mechanistically, low affinity–primed memory CD8$^+$ T cells produced more IL-2 and significantly upregulated IL-2Rα expression during rechallenge. We found that CD45RB^{hi} status was also a stable marker of priming affinity within polyclonal CD8$^+$ T cell populations. Following high-affinity rechallenge, low affinity–primed CD45RB^{hi} cells became CD45RB^{lo}, demonstrating that CD45RB status acts as an affinity-based differentiation switch on CD8$^+$ T cells. Thus, these data establish a novel mechanism by which CD45 isoforms tune low affinity–primed memory CD8$^+$ T cells to become potent secondary effectors following heterologous rechallenge. These findings have direct implications for allogeneic heterologous immunity by demonstrating that despite a lower precursor frequency, low-affinity priming is sufficient to generate memory cells that mediate potent secondary responses against a cross-reactive graft challenge. ***The Journal of Immunology*****, 2016, 196: 2838–2846.**

Following encounter with microbial Ag, T cells can differentiate into memory cells with a multitude of phenotypic profiles to provide long-lasting protection against subsequent encounters with pathogens (1, 2). Memory T cells are recognized as a barrier to many immunomodulation strategies aimed at limiting alloreactive T cell responses (3). One reason is that microbe-elicited T cell memory can cross-react with allogeneic Ag and mediate graft rejection, a process termed allogeneic heterologous immunity (4, 5). In this scenario, memory CD8$^+$ T cells that were primed with microbial Ag can recognize a unique cross-reactive allogeneic Ag. A number of studies have provided evidence of significant cross-reactivity of pathogen-elicited memory CD8$^+$ T cells with allogeneic Ag in mice and humans (4–7).

The affinity of the TCR for Ag is also a critical facet of allogeneic heterologous immunity due to the recognition of the TCR by unique microbial priming and allogeneic rechallenge Ags. Indeed, memory T cells can have high and low affinity for allogeneic Ag (5), and recent work has also demonstrated that allogeneic T cells are suited to recognize a greater number of unique peptide–MHC complexes than conventional T cells, providing strong evidence that allogeneic T cell interactions occur over a range of high and low TCR affinities (8–10). Recently, low-affinity memory T cells have been studied in the context of protective immunity and autoimmunity. However, a specific investigation of the impact of TCR-priming affinity on subsequent phenotype and effector function of memory T cells during heterologous rechallenge has not been conducted.

CD45 is a transmembrane phosphatase that is known to tune proximal T cell signaling cascades via differential expression of multiple isoforms. However, the impact of T cell affinity on CD45 isoform expression and subsequent effector function has not been explored. In this study, we found that low-affinity priming dictates a distinct differentiation program compared with high-affinity priming that is characterized by expression of large CD45 isoforms, denoted as CD45RB^{hi}. A CD45RB^{hi} status enabled low affinity–primed memory CD8$^+$ T cells to proliferate better than high-affinity memory CD8$^+$ T cells in response to a high-affinity graft rechallenge. This study establishes a novel connection between the affinity of CD8$^+$ T cell priming and CD45-mediated T cell tuning, and it provides mechanistic insight into the functionality of low-affinity T cells in transplantation, protective immunity, and autoimmunity.

Materials and Methods

Mice

Male C57BL/6 Ly5.2-Cr (B6.SJL-*Ptprc*^{a} *Pepc*^{b}/BoyJ; CD45.1$^+$, H-2^b) mice were obtained from the National Cancer Institute (Frederick, MD). OT-I (11) transgenic mice (C57BL/6-Tg(TcraTcrb)1100Mjb/J; H-2^b), purchased from Taconic Farms, were bred to Thy1.1$^+$ background at Emory University. Membrane-bound OVA mice (C57BL/6-Tg(CAG-OVA) 916Jen/J; H-2^b), which express membrane-bound N4 OVA under the

*Emory Transplant Center, Atlanta, GA 30322; and †Department of Microbiology and Immunology, Emory University, Atlanta, GA 30322

[1]R.J.M. and R.A. contributed equally to this work.

Received for publication March 16, 2015. Accepted for publication January 12, 2016.

This work was supported by National Institutes of Health Grants R01 AI073707 (to M.L.F.), R01 AI104699 (to M.L.F.), R37 AI040519 (to C.P.L.), T32 AI007610-11 (to S.M.K.), T32 GM08169-23 (to S.M.K.), T32 A1070081 (to S.M.K.), and F30 DK098928-01 (to S.M.K.).

Address correspondence and reprint requests to Dr. Mandy L. Ford, Emory Transplant Center, 101 Woodruff Circle, WMB Suite 5105, Atlanta, GA 30322. E-mail address: mandy.ford@emory.edu

The online version of this article contains supplemental material.

Abbreviations used in this article: APL, altered peptide ligand; 2D, two-dimensional; hnRNPLL, heteronuclear ribonuclear protein L-like; LM-OVA, *Listeria monocytogenes*–expressing OVA; MST, mean survival time; Tm cell, in vitro–primed OT-I cell.

control of the β-actin promoter, were a gift from Dr. Marc Jenkins (University of Minnesota, Minneapolis, MN) (12). All animals were maintained in accordance with Emory University Institutional Animal Care and Use Committee guidelines. All animals were housed in pathogen-free animal facilities at Emory University.

Generation of OT-I primary, memory, and secondary effectors

For adoptive transfers of donor-reactive T cells, Thy1.1$^+$ OT-I mice were processed to single-cell suspension and the frequency of OT-Is was determined by FACS analysis of CD8$^+$Thy1.1$^+$Vα2$^+$ (BD Biosciences). Cells were resuspended in PBS and 1.0×10^4 cells were transferred i.v. into CD45.1$^+$ male hosts. *Listeria monocytogenes* strains engineered to express the OVA-altered peptide ligand epitope (LM-OVA APLs) were provided by Dr. Michael Bevan (University of Washington, Seattle, WA) (13). Mice were infected with 10^4 CFU LM-OVA APL strains i.p. 24 h after adoptive transfer. To generate secondary effectors, at 4 wk following infection mice were immunized with 10 μg N4 OVA (SIINFEKL) peptide (GenScript) in each hind foot pad.

Assessment of in vivo OT-I populations

At primary effector time point day 7 postinfection, CD8$^+$CD44^{hi}Thy1.1$^+$ OT-I cells were identified in the peripheral blood following collection in heparinized capillary tubes and RBC lysis. Primary and secondary effector OT-I cells were identified as CD8$^+$CD19$^-$CD44^{hi}Thy1.1$^+$ from single-cell suspensions. To assess resting OT-I memory cells, at week 4 postinfection (days 28–35), spleen and lymph nodes (popliteal, inguinal, mesenteric, brachial, axial, and cervical) were pooled and enriched for Thy1.1 cells using magnetic beads (14). Briefly, single-cell suspensions were incubated with anti-Thy1.1 PE and anti-PE microbeads (Miltenyi Biotec), followed by enrichment over LS columns. The unbound column flow-through and wash fraction was routinely absent of OT-I cells. Memory OT-I cells were assessed as CD45.2$^+$CD19$^-$CD11c$^-$CD4$^-$CD8$^+$CD44^{hi}Thy1.1$^+$. In some experiments, 200 μl 2 mg/ml BrdU was given i.p. on day 4 after graft, and splenic OT-I cells were enriched for analysis 18 h later. Absolute cell numbers were determined using AccuCheck beads (Invitrogen).

In vitro OVA APL OT-I stimulations

Spleen and mesenteric lymph node cells from OT-I mice were processed to single-cell suspension, and 3×10^6 splenocytes were plated in 24-well plates in complete RPMI 1640 medium supplemented with 0.1 μM OVA APL peptide, 0.1 μg/ml anti-CD28 (37.51, BioLegend), and 10 ng/ml IL-2 (BioLegend) for 3 d. Dead cells were removed using lymphocyte separation medium (CellGro), and cells were cultured in media containing 10 ng/ml IL-15 (BioLegend) overnight, followed by flow cytometry. Cells were restimulated on day 4 following the addition of naive B6 splenocytes at a 1:1 ratio for 5 h in the presence of 0.1 μM OVA APL peptide. For CD45RB cell sorting, Q4 OVA–primed cells were isolated using lymphocyte separation medium and stained with Live/Dead Aqua (Invitrogen), gated on Aqua$^-$CD8$^+$CD44^{hi}Thy1.1$^+$, and sorted as CD45RB^{hi} and CD45RB^{lo} using a FACSAria II (BD Biosciences).

Assessment of polyclonal OVA-specific CD8$^+$ T cells

Mice were infected with 10^4 CFU LM-OVA APL strains i.p. and assessed on days 10–14 postinfection. For N4 OVA–specific tetramer staining, monomers were obtained from the National Institutes of Health Tetramer Core Facility, and 180 μg monomer (90% biotinylation) was tetramerized with streptavidin-allophycocyanin using standard techniques. Tetramer staining was performed on splenic CD3ε$^+$CD19$^-$CD11c$^-$CD8$^+$CD44^{hi} cells for 20–30 min at room temperature at the indicated concentrations.

Skin transplantation

Full-thickness tail and ear skins were transplanted onto the dorsal thorax of recipient mice and secured with adhesive bandages as previously described (15). In some experiments, mice were treated with 500 μg each hamster monoclonal anti-mouse CD154 (MR-1, Bio X Cell) and CTLA-4 Ig or 250 μg anti-CD45RB (HB-220, Bio X Cell) on days 0, 2, 4, and 6 after transplant.

Flow cytometry and intracellular cytokine staining

Single-cell suspensions were stained with anti-CD3, anti-CD8, anti-CD19, anti-CD25, anti-CD44, anti-CD45RB, anti-CD62L, anti-CD69, anti-CD122, anti-CD127, anti-CD11c, anti–PD-1, and anti-Thy1.1 or appropriate isotype control (BD Biosciences or BioLegend) for 15 min at room temperature. For intracellular marker and cytokine staining, cells were incubated for 5 h at 37°C in the presence of 1 μM N4 OVA peptide (GenScript) and 10 μg/ml GolgiPlug (BD Biosciences) and stained for intracellular IL-2, TNF, and IFN-γ following the manufacturers' instructions (BD Biosciences). Assessment of Nur77 (eBioscience) and heteronuclear ribonuclear protein L-like (hnRNPLL; clone TR75-89, Cell Signaling Technology) expression was performed using the Foxp3/transcription factor staining buffer set (eBioscience). hnRNPLL was detected with anti-rabbit F(ab′)$_2$ secondary reagent (Cell Signaling Technology). Data were analyzed using FlowJo software (Tree Star).

Relative two-dimensional affinity measurement of CD8$^+$ T cells

Human RBCs were isolated in accordance with the Institutional Review Board at Emory University. RBCs were coated with Biotin-X-NHS (EMD Millipore) and 0.5 mg/ml streptavidin (Thermo Fisher Scientific) and 1–2 μg N4 OVA or OVA APL H-2K^b monomers with mouse β$_2$-microglobulin (National Institutes of Health Tetramer Core). Monomers cannot bind CD8 due to substitution of the mouse H-2K^b α_3 domain with human HLA-A2 α_3 domain. Monomer bound to RBCs was quantified with anti–N4 OVA K^b PE Ab (25-D1.16; eBioscience) and QuantiBrite beads (BD Biosciences). Naive splenic OT-I T cells were purified using an EasySep mouse CD8$^+$ T cell negative selection kit (Stemcell Technologies), and TCR was quantified by staining with anti-Vα2 PE Ab (B20.1; eBioscience) and QuantiBrite beads. For the relative two-dimensional (2D) affinity of polyclonal CD8$^+$ T cells, splenic CD3ε$^+$CD19$^-$CD8$^+$CD44^{hi} cells from day 10 LM–N4 OVA-infected mice were sorted into CD45RB^{hi} and CD45RB^{lo} populations using a FACSAria II (BD Biosciences), and the TCR was quantified with anti-TCRβ (H57-597; BD Biosciences) and QuantiBrite beads. The micropipette adhesion frequency assay was then performed as previously described (16, 17). In brief, a pMHC-coated RBC and T cell were placed on apposing micropipettes and brought into contact by micromanipulation for a controlled contact area (A_c) and time (t). The T cell was retracted at the end of the contact period, and the presence of adhesion (indicating TCR–pMHC binding) was observed by elongation of the RBC membrane. This TCR–RBC contact was repeated 30 times and the adhesion frequency (P_a) was calculated. The relative 2D affinity (A_cK_m) of each cell that had a P_a of >10% was calculated using the P_a at equilibrium (where $t \rightarrow \infty$) using the following equation: $A_cK_a = \ln[1 - P_a(\infty)]/(m_r m_l)$, where m_r and m_l reflect the receptor (TCR) and ligand (pMHC) densities, respectively.

Statistical analysis

Survival data were plotted on Kaplan–Meier curves and log-rank tests were performed. For analysis of absolute numbers and expression levels, paired or unpaired Student t tests (two-tailed) were performed, where appropriate. Analysis of expression of markers on naive and memory cells was performed using one-way ANOVA with Bonferroni posttest. Analysis of expression of markers by CD45RB expression was performed using two-way repeated measures ANOVA with a Bonferroni posttest. Fold expansion in proliferation of N4 OVA–rechallenged secondary effectors was calculated as absolute number OT-I N4 OVA rechallenge divided by average number resting OT-I. Fold change of CD45RB expression on resting memory versus secondary effectors was calculated as 100 − (% CD45RB^{hi} secondary effector cells/average % CD45RB^{hi} resting memory cells). Percentage maximum of N4 OVA tetramer binding was calculated as (frequency N4 OVA Tet$^+$)/(frequency N4 OVA Tet$^+$ 1:50 dilution) × 100. Comparisons of relative 2D affinity of OVA APLs compared with N4 OVA were performed using one-way ANOVA (Dunnett posttest). Linear correlations of relative 2D affinity were evaluated with mean survival time (MST), CD45RB expression, or EC_{50} values (13). Results were considered significant when $p < 0.05$. All analyses were done using GraphPad Prism software (GraphPad Software).

Results

OVA APL relative 2D affinity correlates with functional avidity

The affinity of TCR interactions during priming impacts naive CD8$^+$ T cell differentiation into effector and memory cells (1, 18, 19). Although many studies have used the OVA-based APLs (13, 20–22), the affinity of the OT-I TCR for many OVA APLs has not been reported. Using a micropipette adhesion assay (17), we measured the relative 2D affinity of OT-I T cells to parental N4 OVA (SIINFEKL) as well as single amino acid substitution APLs Q4 OVA (SIIQFEKL), T4 OVA (SIITFEKL), and V4 OVA (SIIVFEKL). In contrast to functional avidity measurements (13, 22), this technique measures the isolated affinity of the TCR and peptide–MHC binding in the context of physiologic cellular membranes without the con-

tributions of other surface receptors, such as CD8 (16). We found that the 2D affinity of OVA APLs ranged from N4 OVA 3.8×10^{-4} (high affinity) to V4 OVA 1.67×10^{-5} μm^4 (low affinity) (Fig. 1A), representing a 23.9-fold range of affinity (Fig. 1B). This range between N4 and V4 OVA is >10-fold narrower than the reported 680-fold range in relative functional avidity (13). Importantly, we identified a linear relationship between relative functional avidity and 2D affinity ($R^2 = 0.972$, Fig. 1C).

Low affinity–primed memory CD8+ T cells are tuned to generate robust secondary recall responses

During heterologous immunity, T cells primed with high or low affinity for the priming pathogen Ag can cross-react with allogeneic Ag and mediate graft rejection. Thus, we developed an in vivo model to investigate the role that TCR affinity plays in heterologous immunity. We used *L. monocytogenes* strains engineered to express the OT-I epitope N4 OVA or the low-affinity V4 OVA epitopes to generate high or low affinity–primed $CD8^+$ T cell memory, respectively, and then challenged these memory populations with an N4 OVA–expressing skin graft (Fig. 1D). Compared to N4 OVA priming, V4 OVA priming led to an ~80-fold lower frequency of $CD8^+$ OT-I effectors in the blood on day 7 (Supplemental Fig. 1A). Using an enrichment technique to reliably detect and quantify very low frequency OT-I memory T cells (14), we found that high affinity–primed N4 OVA cells and low affinity–primed V4 OVA cells formed memory populations in secondary lymphoid organs (Fig. 1E, Supplemental Fig. 1B). Low affinity–primed V4 OVA cells were found at a 61-fold lower frequency than those primed by N4 OVA (N4 OVA, $8.0 \times 10^4 \pm 3.3 \times 10^4$; V4 OVA, $1.3 \times 10^3 \pm 5.3 \times 10^2$; Fig. 1E). Consistent with the phenotype of high-quality $CD8^+$ memory T cells, both N4 OVA– and V4 OVA–primed memory cells expressed high levels of CD44 and CD127 and low levels of CD69 and granzyme B (Supplemental Fig. 1C). Thus, whereas primary effector proliferation correlates with TCR signal strength, low-affinity priming leads to memory cell formation.

Following challenge with high-affinity N4 OVA skin grafts, high affinity–primed N4 OVA memory cells elicited rejection of grafts with an MST of 17 d (Fig. 1F). Surprisingly, despite a 61-fold lower precursor frequency, low affinity–primed V4 OVA memory cells cross-reacting with graft-expressed high-affinity N4 OVA mediated faster graft rejection (MST of 11 d, $p < 0.0001$, Fig. 1F). Challenge of mice with memory cells primed with either of two additional intermediate-affinity OVA APLs Q4 and T4 resulted in graft rejection kinetics that were faster than high-affinity N4 OVA (Q4 OVA MST of 15.5 d, T4 OVA MST of 14.0 d, Supplemental Fig. 1D). The MST of high-affinity N4 OVA skin graft challenge correlated with the priming affinity (13) (Supplemental Fig. 1D).

We investigated the relative differences in graft rejection kinetics and found that they were the result of differential qualitative TCR signaling or proliferative potential between high and low affinity–primed memory $CD8^+$ T cells. In response to high-affinity N4 OVA rechallenge, high and low affinity–primed memory $CD8^+$ T cells upregulated similar levels of CD69 and Nur77, which report qualitative TCR-mediated signal strength at early time points (22, 23) (Supplemental Fig. 2A, 2B).

On day 5 following N4 OVA skin graft, fewer low-affinity V4 OVA–primed cells were recovered in the draining lymph nodes compared with N4 OVA–primed cells (Fig. 1G). However, low-affinity V4 OVA–primed cells underwent a greater fold expansion (Fig. 1H), and a significantly higher frequency of V4 OVA–primed cells incorporated BrdU on day 5 after graft ($p < 0.0001$, Fig. 1I).

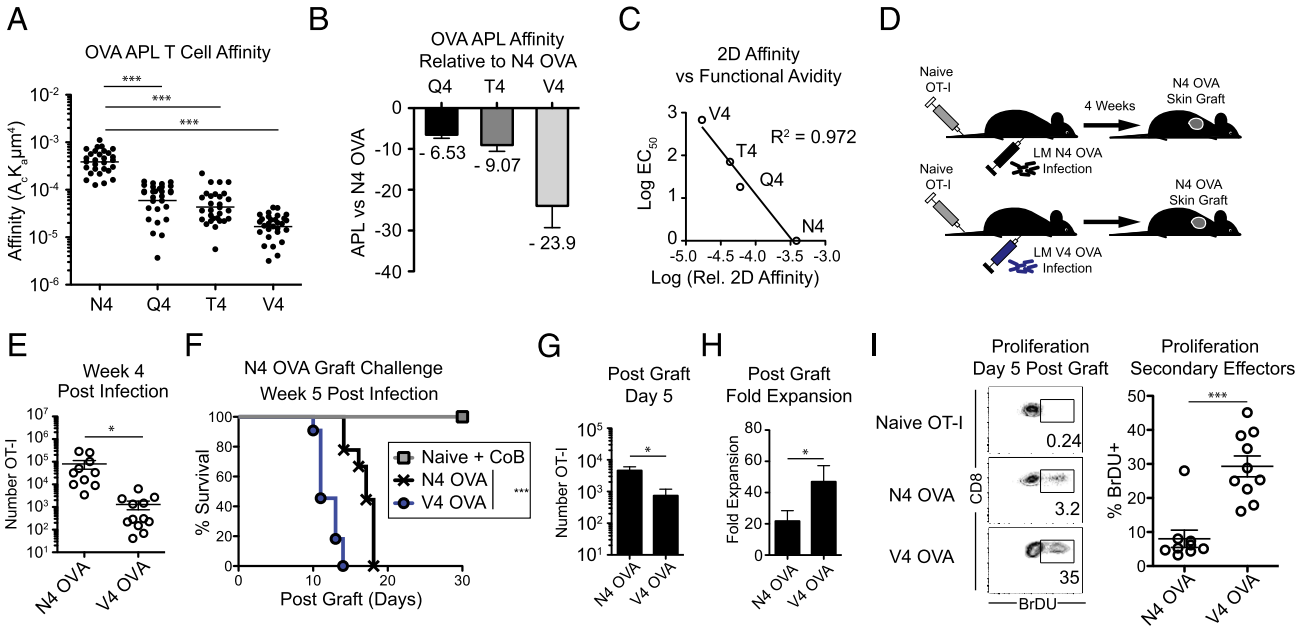

FIGURE 1. Low affinity–primed $CD8^+$ T cells mount potent secondary responses against high-affinity grafts. (**A**–**C**) The relative 2D affinity of naive OT-I T cells to N4 OVA, Q4 OVA, T4 OVA, and V4 OVA H-2^b were measured using a micropipette. (A) Relative 2D affinity of OT-I T cells to N4 OVA and OVA APLs. (B) Fold difference in 2D affinity between N4 OVA and OVA APLs. (C) Linear association between relative 2D affinity and reported relative functional avidity. (**D**–**H**) Naive mice adoptively transferred with 10^4 OT-I T cells were infected the following day with either LM–N4 OVA or LM–V4 OVA. Naive mice or mice containing N4 OVA– or V4 OVA–primed memory OT-I cells were transplanted with N4 OVA skin grafts 5 wk postinfection. (E) Frequency of memory N4-OVA– and V4 OVA–primed memory OT-I cells in pooled secondary lymphoid organs (N4 OVA versus V4 OVA $p < 0.001$). (F) N4 OVA skin graft survival in LM–N4 OVA- or LM–V4 OVA-infected mice. Naive mice were treated with CTLA-4 Ig and anti-CD154 costimulation blockade (N4 OVA versus V4 OVA groups $p < 0.0003$). (G) Number of N4 OVA– or V4 OVA–primed OT-I cells recovered in the draining lymph nodes on day 5 after graft. (H) Fold expansion of N4 OVA– and V4 OVA–primed memory cells from day 0 to day 5 after graft. (**I**) Frequency of $BrDU^+$ cells among N4 OVA– or V4 OVA–primed secondary effectors on day 5 following skin graft, or in ungrafted naive OT-I controls. Data compiled from at least three independent experiments. *$p < 0.05$, ***$p < 0.0001$. CoB, costimulation blockade.

These results could not be attributed to different rates of apoptosis between memory populations (Supplemental Fig. 2C), nor were they due to differences in OVA-specific endogenous $CD8^+$ populations, as similar frequency and absolute number of endogenous $CD8^+$ T cells were N4 OVA specific (Supplemental Fig. 2D). Thus, in response to high-affinity rechallenge, low affinity–primed memory $CD8^+$ T cells can receive strong TCR-mediated activation signals and are poised to undergo greater proliferative responses compared with high affinity–primed memory T cells.

CD45RB is a stable marker of the affinity experience of memory CD8$^+$ T cells

We investigated the mechanism underlying the ability of low affinity–primed V4 OVA memory cells to mediate faster graft rejection and undergo greater proliferation than high affinity–primed N4 OVA memory cells in response to high-affinity graft challenge. CD45 is a transmembrane phosphatase that is critical for TCR signaling. Interestingly, the relative abundance of CD45 isoforms can be used to distinguish T cell differentiation status in mice, as naive $CD8^+$ T cells are $CD45RB^{hi}$ and effector/memory $CD8^+$ T cells downregulate CD45RB to become predominantly $CD45RB^{lo}$ (24).

Given their overall memory cell phenotype compared with high affinity–primed memory cells (13) (Supplemental Fig. 1C), we questioned whether low affinity–primed memory $CD8^+$ T cells became $CD45RB^{lo}$ during effector and memory differentiation. During the primary effector response we found that high affinity–primed N4 OVA effectors downregulated CD45RB (48.9 ± 2.2% $CD45RB^{hi}$, Fig. 2A). Surprisingly, V4 OVA–primed OT-I cells in the blood maintained a predominantly $CD45RB^{hi}$ status compared with high affinity–primed cells (V4 OVA, 68.7 ± 3.6% $CD45RB^{hi}$, $p < 0.001$; Fig. 2A). At memory, the divergent frequency of

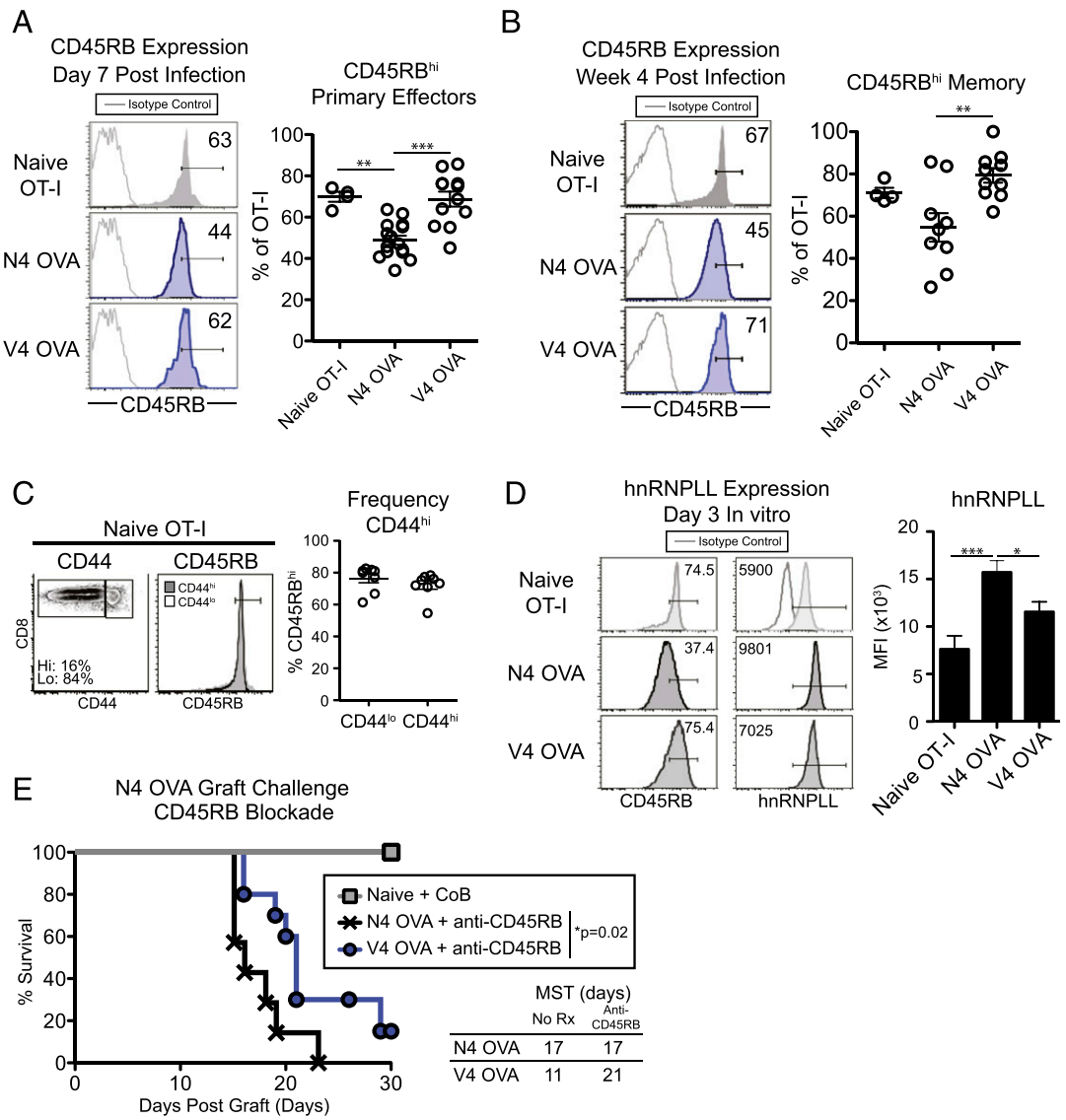

FIGURE 2. Low-affinity memory $CD8^+$ T cells retain a $CD45RB^{hi}$ status. Naive mice adoptively transferred with 10^4 OT-I T cells were infected the following day with either LM–N4 OVA or LM–V4 OVA and memory OT-I T cells and assessed (**A**) in the blood on day 7 or (**B**) in the secondary lymphoid organs 4 wk postinfection. (A) Frequency of $CD45RB^{hi}$ cells on naive or primary effector N4 OVA or V4 OVA T cells. (B) Frequency of $CD45RB^{hi}$ cells among naive OT-I or N4 OVA or V4 OVA memory OT-I cells. (**C**) Frequency of $CD45RB^{hi}$ cells among naive OT-I $CD44^{hi}$ and $CD44^{lo}$ cells. (**D**) hnRNPLL expression in OT-I T cells primed with N4 OVA or Q4 OVA peptide for 3 d in vitro. (**E**) Naive mice or mice containing N4 OVA– or V4 OVA–primed memory OT-I cells were transplanted with N4 OVA skin grafts 5 wk postinfection and treated with anti-CD45RB. Naive mice were treated with CTLA-4 Ig and anti-CD154 costimulation blockade. Data were compiled from two tofour independent experiments. $*p < 0.05$, $**p < 0.01$, $***p < 0.001$. CoB, costimulation blockade.

CD45RB^{hi} cells was maintained in high and low affinity–primed OT-I cells residing in secondary lymphoid tissue (N4 OVA, 54.7 ± 6.76%; V4 OVA, 79.3 ± 3.4%, $p = 0.0064$; Fig. 2B).

A small fraction of naive OT-I cells are CD44^{hi} and have a memory-like phenotype (25). We found that both CD44^{hi} and CD44^{lo} naive OT-I T cell populations were CD45RB^{hi}, indicating that the divergent CD45RB status of OT-I effectors following high- and low-affinity priming was not due to differential expression of CD45RB on naive OT-I T cells prior to adoptive transfer (Fig. 2C). We also investigated the expression of several other molecules that have been shown to modulate TCR signaling. We found no significant difference in expression of Vα2, CD8, or CD5 expression on high and low affinity–primed OT-I cells (Supplemental Fig. 2E).

The mRNA for the gene *PTPRC* undergoes alternative splicing of exons 3, 4, and 5 to generate mature transcripts that encode the extracellular CD45 A, B, and C domains, respectively (24). hnRNPLL has been shown to control inclusion of exons A and C in the *PTPRC* transcript in peripheral CD8$^+$ T cells (26, 27). We questioned whether hnRNPLL was differentially expressed following high- and low-affinity priming, which could reflect the presence of larger CD45 transcripts that contain domains A and/or C. We found that hnRNPLL expression increased following stimulation of OT-I cells with N4 OVA, consistent with a previous report (26). However, hnRNPLL expression was not induced following low-affinity V4 OVA priming (Fig. 2D). Thus, the CD45RB^{hi} status of low affinity–primed cells likely reflects the expression of a greater frequency of large CD45 isoforms that also contain domains A and C.

To determine whether CD45RB expression on low affinity–primed memory CD8$^+$ T cells was functionally important in mediating graft rejection, we treated N4 OVA and V4 OVA memory mice with anti-CD45RB mAb during skin graft rechallenge. Blockade of CD45RB during N4 OVA skin graft challenge did not significantly prolong graft survival in mice containing N4 OVA–primed cells compared with untreated mice (untreated MST 17 d, Fig. 1F; anti-CD45RB MST 17 d, Fig. 2E). However, treatment of mice containing V4 OVA–primed memory CD8$^+$ T cells with anti-CD45RB led to significant prolongation of graft survival (untreated MST 11 d, Fig. 1F; anti-CD45RB MST 21 d, Fig. 2E), demonstrating that CD45RB is functionally important specifically in the context of a secondary recall response mediated by low affinity–primed memory CD8$^+$ T cells. These data reveal that long-lived CD44^{hi} memory T cells can remain predominantly CD45RB^{hi} and that this CD45RB^{hi} status is functionally important during rechallenge.

Low affinity–primed secondary effector cells downregulate CD45RB and produce high levels of IL-2

In light of the finding that low affinity–primed CD8$^+$ memory T cells mount robust secondary recall responses against high-affinity Ag, we investigated the phenotype of high and low affinity–primed secondary effectors. Because skin grafts elicit relatively little expansion of Ag-specific T cells, we rechallenged memory populations with peptide in vivo and assessed T cells in the draining lymph node. Similar to secondary responses after graft, low affinity–primed secondary effectors underwent a 5.3-fold greater expansion than did high affinity–primed secondary populations ($p < 0.0001$, Supplemental Fig. 3A, 3B).

High-affinity N4 OVA peptide rechallenge of N4 OVA–primed memory cells slightly downregulated CD45RB expression (30.2 ± 3.39% CD45RB^{hi}, Fig. 3A). In contrast, V4 OVA–primed memory cells significantly downregulated CD45RB expression during the secondary proliferative response to high-affinity Ag (19.6 ± 1.96% CD45RB^{hi}, Fig. 3A). The loss of CD45RB^{hi} cells was significantly greater in V4 OVA–primed secondary effectors compared with N4 OVA–primed secondary effectors ($p < 0.001$,

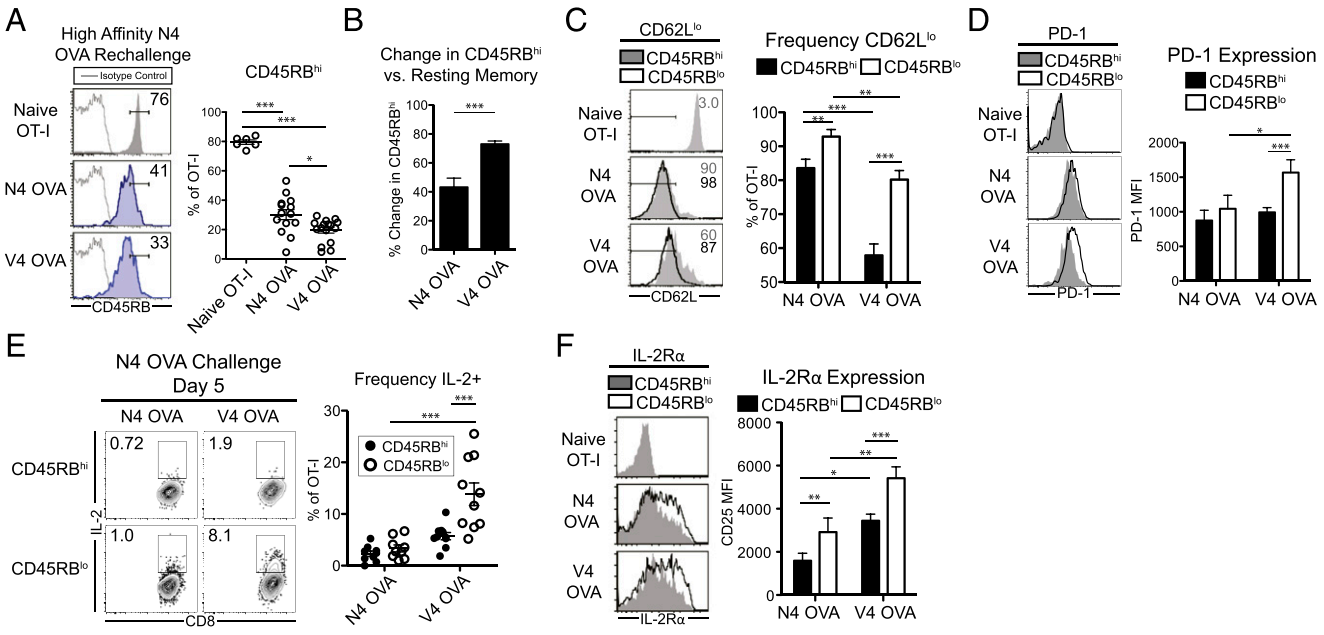

FIGURE 3. Low affinity–primed secondary effectors downregulate CD45RB and have a distinct IL-2–producing effector phenotype. Naive mice adoptively transferred with 10^4 OT-I T cells were infected the following day with either LM-N4 OVA or LM-V4 OVA. Four weeks postinfection, mice were challenged with N4 OVA peptide in the foot pad, and the draining popliteal lymph nodes were assessed 5 d later. (**A**) Frequency of CD45RB^{hi} cells among naive and secondary effector OT-I T cells. (**B**) Relative reduction in CD45RB^{hi} frequency of secondary effector populations compared with resting memory cells. (**C**) Frequency of CD62L^{lo} cells in CD45RB^{hi} and CD45RB^{lo} fractions of secondary effector OT-I cells. (**D**) PD-1 expression in CD45RB^{hi} and CD45RB^{lo} fractions of secondary effector OT-I cells. (**E**) IL-2 expression by secondary effectors following brief N4 peptide restimulation in CD45RB^{hi} and CD45RB^{low} fractions. (**F**) IL-2Rα (CD25) expression in CD45RB^{hi} and CD45RB^{lo} fractions of secondary effector OT-I cells. Data were compiled from two to three independent experiments. *$p < 0.05$, **$p < 0.01$, ***$p < 0.001$.

Fig. 3B). Low affinity–primed secondary effectors also downregulated CD45RB following N4 OVA skin graft challenge (Supplemental Fig. 3C). A large proportion of both secondary effector populations were CD62L^{lo} (Fig. 3C). However, a greater frequency of both N4 OVA and V4 OVA CD45RB^{lo} secondary effectors had a CD62L^{lo} effector phenotype compared with their respective CD45RB^{hi} populations (N4 OVA and V4 OVA $p < 0.001$, Fig. 3C). Interestingly, a slightly smaller frequency of CD62L^{lo} cells was contained within the V4 OVA CD45RB^{lo} population compared with the N4 OVA CD45RB^{lo} population ($p < 0.01$, Fig. 3C). The cosignaling receptor PD-1 has been shown to be a marker of cumulative effector signal strength on effector CD8$^+$ T cells and to correlate with CD62L expression (28). PD-1 was significantly upregulated in CD45RB^{lo} fraction of V4 OVA–primed cells (Fig. 3D), demonstrating that this population perceives strong TCR signals.

IL-2 is a critical cytokine for CD8$^+$ T cell secondary responses (29). Consistent with previous published results (30, 31), a low frequency of N4 OVA–primed secondary effectors produced IL-2 (Fig. 3E). In contrast, we found that a significantly greater proportion of V4 OVA–primed CD45RB^{lo} cells produced IL-2 (Fig. 3E). High IL-2 production was specific to low affinity–primed CD45RB^{lo} secondary effectors during N4 OVA rechallenge, as high and low affinity–primed day 7 effectors produced similarly low levels of IL-2 (Supplemental Fig. 3D). In contrast, V4 OVA–primed CD45RB^{lo} populations did not possess greater frequencies of IFN-γ^+ or TNF$^+$ cells compared with CD45RB^{hi} populations following high-affinity rechallenge (Supplemental Fig. 3E).

IL-2 signaling can induce the expression of the high-affinity IL-2Rα-chain (CD25) (32), and high IL-2Rα expression is associated with differentiated effector cells (32–34). We found that V4 OVA–primed CD45RB^{lo} cells expressed significantly higher levels of IL-2Rα compared with both CD45RB^{hi} cells and N4 OVA–primed CD45RB^{lo} cells (N4 OVA CD45RB^{hi} versus CD45RB^{lo} $p < 0.001$, CD45RB^{lo} N4 OVA versus V4 OVA $p < 0.01$, Fig. 3F). High expression of the IL-2Rβ-chain, CD122, can confer sensitivity to IL-15 signaling in memory T cells, whereas lower expression is associated with IL-2 sensitivity and effector T cells (34, 35). We found that high-affinity N4 OVA–primed secondary effectors expressed similar levels of IL-2Rβ (Supplemental Fig. 3F). Among low-affinity V4 OVA–primed secondary effectors, however, CD45RB^{lo} cells expressed significantly lower IL-2Rβ levels than did CD45RB^{hi} cells ($p < 0.01$, Supplemental Fig. 3F). Taken together, these results demonstrate that low affinity–primed CD45RB^{lo} secondary effectors effectively switch into a distinct effector-like phenotype characterized by high IL-2 production, high expression of IL-2Rα, and effector IL-2Rβ expression.

High CD45RB expression tunes CD8$^+$ T cells to respond to heterologous Ag rechallenge

To control for priming conditions and cell numbers encountered after priming with *Listeria* strains in vivo, we investigated CD45RB expression on in vitro–primed OT-I cells (Tm cells). Following in vitro priming of OT-I cells with OVA APLs, we found that Tm cells similarly upregulated CD44 expression but that CD45RB expression correlated inversely with priming affinity (Fig. 4A), consistent with in vivo–derived effector and memory CD8$^+$ T cells (Fig. 2A, 2B).

We investigated whether the differential expression of CD45 isoforms conferred a qualitative TCR signaling advantage by

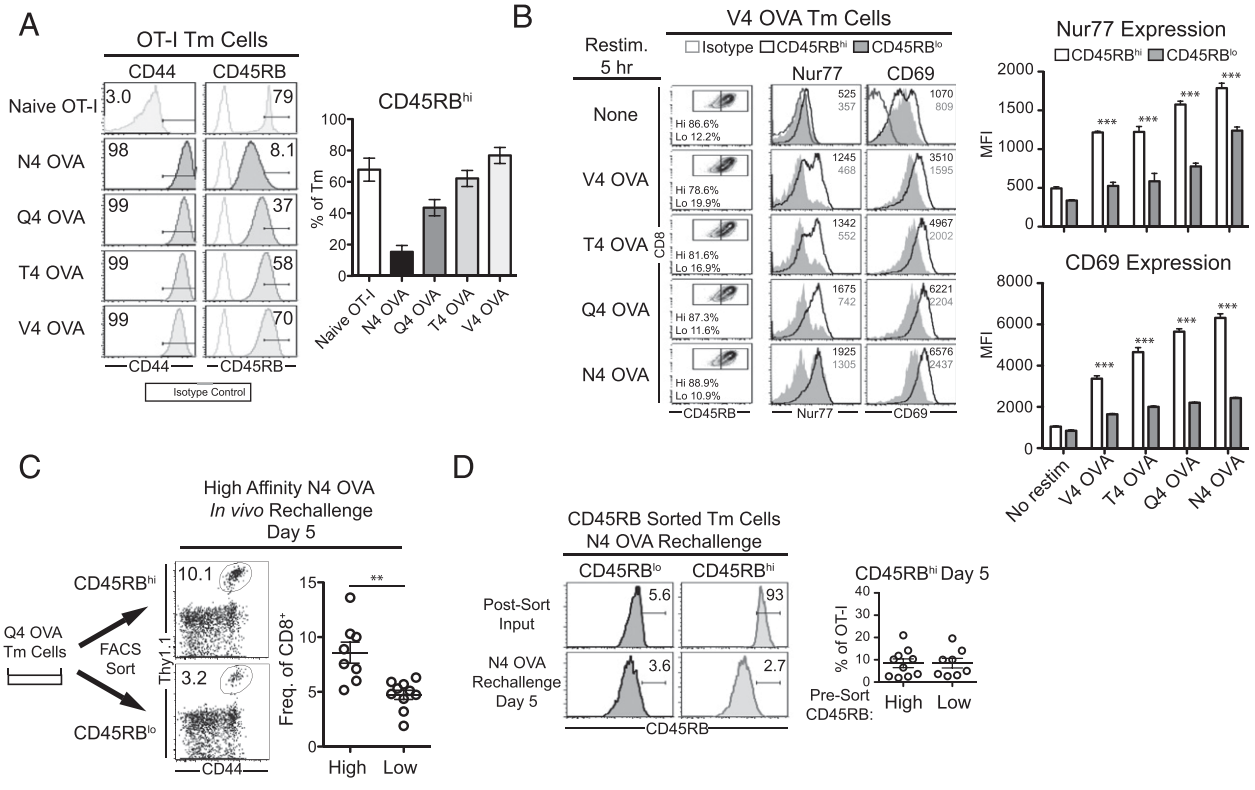

FIGURE 4. High CD45RB expression tunes low affinity–primed memory CD8$^+$ T cells for heterologous rechallenge responses. OT-I T cells were activated in vitro with N4 OVA, Q4 OVA, T4 OVA, or V4 OVA peptide for 4 d. (**A**) Expression of CD44 and CD45RB on OVA APL Tm cells. (**B**) V4 OVA APL Tm cells were restimulated for 5 h with N4 OVA, Q4 OVA, T4 OVA, or V4 OVA peptide and Nur77 and CD69 expression was assessed. (**C** and **D**) Q4 OVA–primed OT-I cells were sorted into CD45RB^{hi} and CD45RB^{lo} populations and adoptively transferred into naive congenic hosts and rechallenged with N4 OVA peptide. (C) The frequency of Q4 OVA cells was assessed 5 d following rechallenge. (D) Expression of CD45RB on Q4 OVA Tm cells before and after rechallenge with N4 OVA peptide for 5 d. Data were compiled from two to three independent experiments. $^{**}p < 0.01$, $^{***}p < 0.001$.

assessing the expression of CD69 and Nur77 in CD45RB^{hi} V4 OVA–primed Tm cells restimulated with OVA APL ligands. After a brief 5-h restimulation, CD45RB expression did not change in these cells (Fig. 4B). We found that the expression of both Nur77 and CD69 was significantly greater in CD45RB^{hi} cells compared with CD45RB^{lo} cells following stimulation with N4 OVA or each OVA APL (Fig. 4B), demonstrating that CD45RB^{hi} cells received qualitatively stronger TCR activation signals compared with CD45RB^{lo} cells.

To investigate whether high CD45RB status is sufficient to confer enhanced recall potential during secondary challenge, we sorted CD45RB^{hi} and CD45RB^{lo} OT-I cells elicited by Q4 OVA priming and rechallenged them with N4 OVA peptide in naive congenic hosts. With this experimental setup, CD45RB^{hi} and CD45RB^{lo} cells encounter identical priming conditions and are rechallenged at identical precursor frequencies. CD45RB^{hi} cells proliferated to a significantly greater number than did CD45RB^{lo} cells ($p = 0.0012$, Fig. 4C). Similar to in vivo low affinity–primed CD45RB^{hi} memory T cells that become CD45RB^{lo} following secondary rechallenge with high-affinity Ag (Fig. 3A), both CD45RB^{hi} and CD45RB^{lo} input populations were predominantly CD45RB^{lo} 5 d following restimulation (Fig. 4D), demonstrating that CD45RB^{hi} cells downregulate expression of CD45RB on a per cell basis in response to high-affinity rechallenge. Taken together, these data demonstrate that a CD45RB^{hi} status is sufficient to confer a qualitatively greater activation signal and a proliferative advantage on low affinity–primed CD8$^+$ T cells and that CD45RB status is a marker of the affinity experience of memory and secondary effector cells.

Polyclonal low-affinity CD8$^+$ T cells express high levels of CD45RB

To determine whether these findings in TCR transgenic CD8$^+$ T cells apply to polyclonal CD8$^+$ T cell populations, we investigated the ability of CD45RB to distinguish the affinity experience of polyclonal CD8$^+$ T cells. In mice infected with LM-OVA, polyclonal populations of naive CD8$^+$ T cells and activated non–N4 OVA-specific CD8$^+$ effectors were predominantly CD45RB^{hi} (90.1 $\pm$ 1.5 and 74.6 $\pm$ 1.36% CD45RB^{hi}, respectively), whereas polyclonal Ag-specific CD8$^+$ T cell effectors display a range of CD45RB expression (23.8 $\pm$ 1.55% CD45RB^{hi}, Fig. 5A). These data suggest that CD45RB expression reflects the range of priming affinities of polyclonal CD8$^+$ T cells for a given Ag.

We investigated the affinity of activated CD8$^+$ T cells based on CD45RB status using 2D affinity measurements. We measured the relative 2D affinity of sorted OVA-specific CD44^{hi} CD45RB^{hi} and CD45RB^{lo} populations from LM-OVA–infected mice (Supplemental Fig. 4A). We found that CD45RB^{hi} cells had ~10-fold lower 2D relative affinity compared with CD45RB^{lo} cells ($p = 0.0001$, Fig. 5B). Tetramer binding can also be used to delineate relative affinity of T cell populations, as low-affinity cells do not efficiently bind tetramer compared with high-affinity cells (17). We found that compared with CD8$^+$CD44^{hi} CD45RB^{hi} cells, CD44^{hi}CD45RB^{lo} cells bound tetramer more effectively at lower concentrations (Fig. 5C, Supplemental Fig. 4B). Compared to CD45RB^{lo} cells, CD45RB^{hi} cells expressed similar levels of CD3ε and slightly higher CD8 coreceptor (Supplemental Fig. 4C), thus demonstrating that differential expression of TCR or CD8 coreceptor do not account for tetramer binding avidity of CD45RB^{hi} and CD45RB^{lo} cells. Thus, these data demonstrate that in a polyclonal population of CD44^{hi} CD8$^+$ T cells, a CD45RB^{hi} status denotes cells primed with lower affinity than CD45RB^{lo} cells.

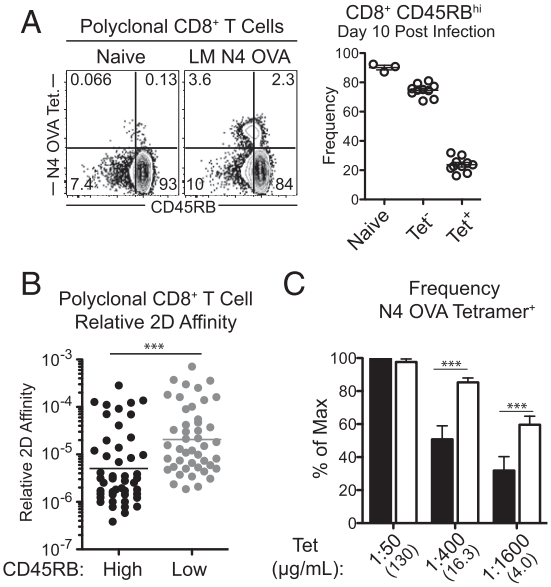

FIGURE 5. Polyclonal CD8$^+$ T cells express CD45RB^{hi}. Naive B6 mice were infected with LM–N4 OVA and splenic CD8$^+$ T cells were assessed 10–14 d later. (**A**) CD45RB expression on tetramer-stained N4 OVA–specific CD8$^+$ T cells. (**B**) Relative 2D affinity of CD45RB^{hi} and CD45RB^{lo} CD8$^+$CD44^{hi} T cells. (**C**) Frequency of tetramer staining among CD45RB^{hi} and CD45RB^{lo} fractions of CD8$^+$CD44^{hi} T cells. Data were compiled from two to three independent experiments. ***$p < 0.001$.

Discussion

In this study, we establish a novel role for CD45 in tuning low affinity–primed memory CD8$^+$ T cells to become potent secondary effectors during heterologous rechallenge. Although it is appreciated that high-affinity memory CD8$^+$ T cells can mediate graft rejection (36, 37), this study specifically addresses the contribution of TCR priming affinity to the function of memory T cells that are directed against a graft. In general, the affinities for allogeneic Ag and foreign microbial Ag are recognized as having a similar range of affinities that is >10-fold (5). In the context of heterologous immunity, a recent study that measured the affinity of a human TCR for both its viral cognate Ag and a cross-reactive alloantigen reported an ~15-fold higher affinity for allogeneic Ag than for the viral epitope (38). In our model, we found a 23.9-fold difference in affinity between N4 OVA and V4 OVA for the OT-I TCR, a magnitude that is in line with both the known range of T cell recognition of allogeneic Ag as well as with microbe-specific T cells that cross-react with allogeneic Ag. Thus, this model recapitulates a critical facet of heterologous immunity by eliciting memory CD8$^+$ T cells with distinct priming affinities in the context of a pathogen that subsequently recognize a related, but not identical, Ag presented in the context of a transplant.

Although the importance of CD45 for immune homeostasis and signaling has been well studied, this study provides a novel physiologic context for CD45-mediated tuning by linking CD8$^+$ TCR priming affinity and CD45RB expression on memory and secondary effector T cells. We found that low affinity–primed cells maintain a CD45RB^{hi} status, which has previously been described only on naive CD8$^+$ T cells. CD45RB was stably expressed at high levels on fully differentiated CD44^{hi} TCR transgenic and polyclonal memory CD8$^+$ T cells following low-affinity priming. The maintenance of a CD45RB^{hi} status was associated with lower expression of hnRNPLL, which suggests that low affinity–primed CD45RB^{hi} CD8$^+$ T cells may express a high frequency of multiple large CD45 isoforms. This difference in

hnRNPLL expression, however, is likely not the only mechanism of differential CD45 isoform usage following low-affinity priming, as hnRNPLL does not control the inclusion of the B domain in peripheral $CD8^+$ T cells (26). Expression of other molecules that are known to tune T cell signaling, including CD8 and CD5, was similar on high and low affinity–primed memory cells. Expression of Nur77 and CD69 have been shown to correlate with priming affinity (13, 22, 23). However, the expression of these markers, as well as functional avidity measured by IFN-γ production, rapidly changes following stimulation (13, 22, 23). Thus, in conjunction with CD44 expression, high CD45RB expression is a novel and stable marker by which low affinity–primed $CD8^+$ memory T cells can be identified.

Previous in vitro work has demonstrated that large CD45 isoforms tune T cells for stronger proximal TCR signaling by undergoing less inhibitory dimerization than do smaller isoforms (24, 39). Consistent with the ability of larger CD45RABC isoform to mediate greater calcium flux compared with CD45RO (39), we demonstrate that low affinity–primed memory and $CD45RB^{hi}$ cells receive greater cumulative TCR signal strength (as assessed by upregulation of Nur77 and CD69) and are poised to undergo greater proliferative and effector responses compared with $CD45RB^{lo}$ cells. Many investigations of the consequences of altered TCR signaling potency have focused on Ag density or genetically attenuated TCR signaling (18, 40–44). However, a recent study elegantly demonstrated that TCR binding affinity and Ag density induce broadly distinct gene expression profiles (45). Thus, the role of CD45 tuning represents a previously unappreciated mechanism by which TCR priming affinity dictates the differentiation program of memory $CD8^+$ T cells during heterologous rechallenge.

These data suggest a model in which CD45RB defines an affinity-based differentiation switch on $CD8^+$ T cells, as low-affinity priming enables proliferation and effector functions along with a $CD45RB^{hi}$ status similar to naive T cells. Following high-affinity rechallenge, low affinity–primed $CD45RB^{hi}$ memory cells differentiate into $CD45RB^{lo}$ secondary effectors with a distinct phenotype characterized by high PD-1 and CD25 expression, increased IL-2 production, and lower CD122 expression. Whereas PD-1 is a marker of exhaustion on $CD8^+$ memory T cells following chronic Ag exposure, its expression is also associated with recent Ag experience in effector $CD8^+$ T cells (28). It remains to be seen whether PD-1 is functioning in a costimulatory or coinhibitory capacity on secondary effectors under these conditions. This prominent IL-2 signaling phenotype was not a general characteristic of high-affinity priming, as N4 OVA and V4 OVA primary effectors expressed similarly low levels of IL-2. Recent work revealed that IL-2 signals are critical for secondary effector $CD8^+$ responses (29, 46) and that CD25 is a marker of terminally differentiated effectors (32, 33). Our data now identify TCR affinity as a driver of an IL-2–dependent memory $CD8^+$ phenotype, and it extends previous work establishing the requirement of IL-2 for secondary recall responses by revealing that low affinity–primed $CD8^+$ secondary effectors produce significant amounts of IL-2.

Recently, considerable evidence has been presented that pathogen-specific T cells can cross-react with allogeneic Ag. In humans, one recent study found that nearly half of viral-specific T cell clones were cross-reactive with allogeneic Ag (6) and 15 individual TCRs that recognize pathogen–allogeneic Ag combinations have been characterized (5, 38). In mice, lymphocytic choriomeningitis virus infection generates memory $CD8^+$ T cells that cross-react with allogeneic Ag and mediate graft rejection (4, 7, 47). However, in addition to single TCR cross-reactivity with allogeneic Ag, dual TCR T cells may also play a role in heterologous immunity against allogeneic Ag (48–51), and it is likely that both cross-reactivity and dual TCR expression contribute to heterologous immunity in polyclonal populations. In this model, we can assess the relative contribution of TCR affinity to memory T cell function in the context of a skin graft, but we cannot assess the relative contribution of additional mechanisms of heterologous immunity within polyclonal T cell populations.

In the context of protective immunity, the ability of low-affinity priming to form memory and undergo robust secondary responses to heterologous rechallenge represents a means of maintaining clonal diversity and protection against encounter with diverse pathogens. However, following transplantation this phenomenon represents a potentially potent driver of allogeneic T cell responses and a barrier to successful immunomodulation. The contribution of low-affinity memory T cells to heterologous immunity provides new rationale for the therapeutic targeting of CD45RB to prevent pathogenic T cell responses, a strategy that has shown promise in preclinical murine (52–54) and nonhuman primate transplantation models (55–57). Collectively, these data highlight the importance of the pathogen priming history of an individual in shaping the potentially pathogenic memory T cell repertoire in settings of allogeneic heterologous immunity and autoimmunity.

Acknowledgments

We thank Dr. Michael Bevan for the contribution of LM-OVA APL strains, Aaron Rae and the Emory and Children's Pediatric Research Flow Cytometry Core for FACS sorting, and Dr. Jonathan Maltzman for critical reading of the manuscript.

Disclosures

The authors have no financial conflicts of interest.

References

1. Kaech, S. M., and W. Cui. 2012. Transcriptional control of effector and memory CD8+ T cell differentiation. *Nat. Rev. Immunol.* 12: 749–761.
2. Jameson, S. C., and D. Masopust. 2009. Diversity in T cell memory: an embarrassment of riches. *Immunity* 31: 859–871.
3. Ford, M. L., and C. P. Larsen. 2010. Overcoming the memory barrier in tolerance induction: molecular mimicry and functional heterogeneity among pathogen-specific T-cell populations. *Curr. Opin. Organ Transplant.* 15: 405–410.
4. Adams, A. B., M. A. Williams, T. R. Jones, N. Shirasugi, M. M. Durham, S. M. Kaech, E. J. Wherry, T. Onami, J. G. Lanier, K. E. Kokko, et al. 2003. Heterologous immunity provides a potent barrier to transplantation tolerance. *J. Clin. Invest.* 111: 1887–1895.
5. Smith, C., J. J. Miles, and R. Khanna. 2012. Advances in direct T-cell alloreactivity: function, avidity, biophysics and structure. *Am. J. Transplant.* 12: 15–26.
6. Amir, A. L., L. J. D'Orsogna, D. L. Roelen, M. M. van Loenen, R. S. Hagedoorn, R. de Boer, M. A. van der Hoorn, M. G. Kester, I. I. Doxiadis, II, J. H. Falkenburg, et al. 2010. Allo-HLA reactivity of virus-specific memory T cells is common. *Blood* 115: 3146–3157.
7. Brehm, M. A., K. A. Daniels, B. Priyadharshini, T. B. Thornley, D. L. Greiner, A. A. Rossini, and R. M. Welsh. 2010. Allografts stimulate cross-reactive virus-specific memory CD8 T cells with private specificity. *Am. J. Transplant.* 10: 1738–1748.
8. Felix, N. J., D. L. Donermeyer, S. Horvath, J. J. Walters, M. L. Gross, A. Suri, and P. M. Allen. 2007. Alloreactive T cells respond specifically to multiple distinct peptide-MHC complexes. *Nat. Immunol.* 8: 388–397.
9. Morris, G. P., P. P. Ni, and P. M. Allen. 2011. Alloreactivity is limited by the endogenous peptide repertoire. *Proc. Natl. Acad. Sci. USA* 108: 3695–3700.
10. Falkenburg, W. J., J. J. Melenhorst, M. van de Meent, M. G. Kester, P. Hombrink, M. H. Heemskerk, R. S. Hagedoorn, E. Gostick, D. A. Price, J. H. Falkenburg, et al. 2011. Allogeneic HLA-A*02-restricted WT1-specific T cells from mismatched donors are highly reactive but show off-target promiscuity. *J. Immunol.* 187: 2824–2833.
11. Hogquist, K. A., S. C. Jameson, W. R. Heath, J. L. Howard, M. J. Bevan, and F. R. Carbone. 1994. T cell receptor antagonist peptides induce positive selection. *Cell* 76: 17–27.
12. Ehst, B. D., E. Ingulli, and M. K. Jenkins. 2003. Development of a novel transgenic mouse for the study of interactions between CD4 and CD8 T cells during graft rejection. *Am. J. Transplant.* 3: 1355–1362.
13. Zehn, D., S. Y. Lee, and M. J. Bevan. 2009. Complete but curtailed T-cell response to very low-affinity antigen. *Nature* 458: 211–214.

14. Moon, J. J., H. H. Chu, J. Hataye, A. J. Pagán, M. Pepper, J. B. McLachlan, T. Zell, and M. K. Jenkins. 2009. Tracking epitope-specific T cells. *Nat. Protoc.* 4: 565–581.
15. Trambley, J., A. W. Bingaman, A. Lin, E. T. Elwood, S. Y. Waitze, J. Ha, M. M. Durham, M. Corbascio, S. R. Cowan, T. C. Pearson, and C. P. Larsen. 1999. Asialo GM1$^+$ CD8$^+$ T cells play a critical role in costimulation blockade-resistant allograft rejection. *J. Clin. Invest.* 104: 1715–1722.
16. Huang, J., V. I. Zarnitsyna, B. Liu, L. J. Edwards, N. Jiang, B. D. Evavold, and C. Zhu. 2010. The kinetics of two-dimensional TCR and pMHC interactions determine T-cell responsiveness. *Nature* 464: 932–936.
17. Sabatino, J. J., Jr., J. Huang, C. Zhu, and B. D. Evavold. 2011. High prevalence of low affinity peptide-MHC II tetramer-negative effectors during polyclonal CD4+ T cell responses. *J. Exp. Med.* 208: 81–90.
18. Corse, E., R. A. Gottschalk, and J. P. Allison. 2011. Strength of TCR-peptide/MHC interactions and in vivo T cell responses. *J. Immunol.* 186: 5039–5045.
19. Zehn, D., C. King, M. J. Bevan, and E. Palmer. 2012. TCR signaling requirements for activating T cells and for generating memory. *Cell. Mol. Life Sci.* 69: 1565–1575.
20. King, C. G., S. Koehli, B. Hausmann, M. Schmaler, D. Zehn, and E. Palmer. 2012. T cell affinity regulates asymmetric division, effector cell differentiation, and tissue pathology. *Immunity* 37: 709–720.
21. Knudson, K. M., N. P. Goplen, C. A. Cunningham, M. A. Daniels, and E. Teixeiro. 2013. Low-affinity T cells are programmed to maintain normal primary responses but are impaired in their recall to low-affinity ligands. *Cell Reports* 4: 554–565.
22. Daniels, M. A., E. Teixeiro, J. Gill, B. Hausmann, D. Roubaty, K. Holmberg, G. Werlen, G. A. Holländer, N. R. Gascoigne, and E. Palmer. 2006. Thymic selection threshold defined by compartmentalization of Ras/MAPK signalling. *Nature* 444: 724–729.
23. Moran, A. E., K. L. Holzapfel, Y. Xing, N. R. Cunningham, J. S. Maltzman, J. Punt, and K. A. Hogquist. 2011. T cell receptor signal strength in Treg and iNKT cell development demonstrated by a novel fluorescent reporter mouse. *J. Exp. Med.* 208: 1279–1289.
24. Hermiston, M. L., Z. Xu, and A. Weiss. 2003. CD45: a critical regulator of signaling thresholds in immune cells. *Annu. Rev. Immunol.* 21: 107–137.
25. Lee, Y. J., S. C. Jameson, and K. A. Hogquist. 2011. Alternative memory in the CD8 T cell lineage. *Trends Immunol.* 32: 50–56.
26. Wu, Z., X. Jia, L. de la Cruz, X. C. Su, B. Marzolf, P. Troisch, D. Zak, A. Hamilton, B. Whittle, D. Yu, et al. 2008. Memory T cell RNA rearrangement programmed by heterogeneous nuclear ribonucleoprotein hnRNPLL. *Immunity* 29: 863–875.
27. Oberdoerffer, S., L. F. Moita, D. Neems, R. P. Freitas, N. Hacohen, and A. Rao. 2008. Regulation of CD45 alternative splicing by heterogeneous ribonucleoprotein, hnRNPLL. *Science* 321: 686–691.
28. Obar, J. J., and L. Lefrançois. 2010. Early signals during CD8 T cell priming regulate the generation of central memory cells. *J. Immunol.* 185: 263–272.
29. Williams, M. A., A. J. Tyznik, and M. J. Bevan. 2006. Interleukin-2 signals during priming are required for secondary expansion of CD8$^+$ memory T cells. *Nature* 441: 890–893.
30. Wherry, E. J., V. Teichgräber, T. C. Becker, D. Masopust, S. M. Kaech, R. Antia, U. H. von Andrian, and R. Ahmed. 2003. Lineage relationship and protective immunity of memory CD8 T cell subsets. *Nat. Immunol.* 4: 225–234.
31. Rutishauser, R. L., G. A. Martins, S. Kalachikov, A. Chandele, I. A. Parish, E. Meffre, J. Jacob, K. Calame, and S. M. Kaech. 2009. Transcriptional repressor Blimp-1 promotes CD8$^+$ T cell terminal differentiation and represses the acquisition of central memory T cell properties. *Immunity* 31: 296–308.
32. Pipkin, M. E., J. A. Sacks, F. Cruz-Guilloty, M. G. Lichtenheld, M. J. Bevan, and A. Rao. 2010. Interleukin-2 and inflammation induce distinct transcriptional programs that promote the differentiation of effector cytolytic T cells. *Immunity* 32: 79–90.
33. Kalia, V., S. Sarkar, S. Subramaniam, W. N. Haining, K. A. Smith, and R. Ahmed. 2010. Prolonged interleukin-2Rα expression on virus-specific CD8$^+$ T cells favors terminal-effector differentiation in vivo. *Immunity* 32: 91–103.
34. Boyman, O., and J. Sprent. 2012. The role of interleukin-2 during homeostasis and activation of the immune system. *Nat. Rev. Immunol.* 12: 180–190.
35. Intlekofer, A. M., N. Takemoto, E. J. Wherry, S. A. Longworth, J. T. Northrup, V. R. Palanivel, A. C. Mullen, C. R. Gasink, S. M. Kaech, J. D. Miller, et al. 2005. Effector and memory CD8$^+$ T cell fate coupled by T-bet and eomesodermin. *Nat. Immunol.* 6: 1236–1244.
36. Kitchens, W. H., D. Haridas, M. E. Wagener, M. Song, A. D. Kirk, C. P. Larsen, and M. L. Ford. 2012. Integrin antagonists prevent costimulatory blockade-resistant transplant rejection by CD8$^+$ memory T cells. *Am. J. Transplant.* 12: 69–80.
37. Ford, M. L., B. H. Koehn, M. E. Wagener, W. Jiang, S. Gangappa, T. C. Pearson, and C. P. Larsen. 2007. Antigen-specific precursor frequency impacts T cell proliferation, differentiation, and requirement for costimulation. *J. Exp. Med.* 204: 299–309.
38. Macdonald, W. A., Z. Chen, S. Gras, J. K. Archbold, F. E. Tynan, C. S. Clements, M. Bharadwaj, L. Kjer-Nielsen, P. M. Saunders, M. C. Wilce, et al. 2009. T cell allorecognition via molecular mimicry. *Immunity* 31: 897–908.
39. Xu, Z., and A. Weiss. 2002. Negative regulation of CD45 by differential homodimerization of the alternatively spliced isoforms. *Nat. Immunol.* 3: 764–771.
40. Teixeiro, E., M. A. Daniels, S. E. Hamilton, A. G. Schrum, R. Bragado, S. C. Jameson, and E. Palmer. 2009. Different T cell receptor signals determine CD8$^+$ memory versus effector development. *Science* 323: 502–505.
41. Wherry, E. J., K. A. Puorro, A. Porgador, and L. C. Eisenlohr. 1999. The induction of virus-specific CTL as a function of increasing epitope expression: responses rise steadily until excessively high levels of epitope are attained. *J. Immunol.* 163: 3735–3745.
42. Smith-Garvin, J. E., J. C. Burns, M. Gohil, T. Zou, J. S. Kim, J. S. Maltzman, E. J. Wherry, G. A. Koretzky, and M. S. Jordan. 2010. T-cell receptor signals direct the composition and function of the memory CD8$^+$ T-cell pool. *Blood* 116: 5548–5559.
43. Wiehagen, K. R., E. Corbo, M. Schmidt, H. Shin, E. J. Wherry, and J. S. Maltzman. 2010. Loss of tonic T-cell receptor signals alters the generation but not the persistence of CD8+ memory T cells. *Blood* 116: 5560–5570.
44. Wherry, E. J., M. J. McElhaugh, and L. C. Eisenlohr. 2002. Generation of CD8$^+$ T cell memory in response to low, high, and excessive levels of epitope. *J. Immunol.* 168: 4455–4461.
45. Gottschalk, R. A., M. M. Hathorn, H. Beuneu, E. Corse, M. L. Dustin, G. Altan-Bonnet, and J. P. Allison. 2012. Distinct influences of peptide-MHC quality and quantity on in vivo T-cell responses. *Proc. Natl. Acad. Sci. USA* 109: 881–886.
46. Feau, S., R. Arens, S. Togher, and S. P. Schoenberger. 2011. Autocrine IL-2 is required for secondary population expansion of CD8$^+$ memory T cells. *Nat. Immunol.* 12: 908–913.
47. Brehm, M. A., T. G. Markees, K. A. Daniels, D. L. Greiner, A. A. Rossini, and R. M. Welsh. 2003. Direct visualization of cross-reactive effector and memory allo-specific CD8 T cells generated in response to viral infections. *J. Immunol.* 170: 4077–4086.
48. Ni, P. P., B. Solomon, C. S. Hsieh, P. M. Allen, and G. P. Morris. 2014. The ability to rearrange dual TCRs enhances positive selection, leading to increased Allo- and Autoreactive T cell repertoires. *J. Immunol.* 193: 1778–1786.
49. Morris, G. P., G. L. Uy, D. Donermeyer, J. F. Dipersio, and P. M. Allen. 2013. Dual receptor T cells mediate pathologic alloreactivity in patients with acute graft-versus-host disease. *Sci. Transl. Med.* 5: 188ra74.
50. Morris, G. P., and P. M. Allen. 2009. Cutting edge: highly alloreactive dual TCR T cells play a dominant role in graft-versus-host disease. *J. Immunol.* 182: 6639–6643.
51. Padovan, E., G. Casorati, P. Dellabona, S. Meyer, M. Brockhaus, and A. Lanzavecchia. 1993. Expression of two T cell receptor alpha chains: dual receptor T cells. *Science* 262: 422–424.
52. Gagliani, N., S. Gregori, T. Jofra, A. Valle, A. Stabilini, D. M. Rothstein, M. Atkinson, M. G. Roncarolo, and M. Battaglia. 2011. Rapamycin combined with anti-CD45RB mAb and IL-10 or with G-CSF induces tolerance in a stringent mouse model of islet transplantation. *PLoS One* 6: e28434.
53. Gagliani, N., T. Jofra, A. Valle, A. Stabilini, C. Morsiani, S. Gregori, S. Deng, D. M. Rothstein, M. Atkinson, M. Kamanaka, et al. 2013. Transplant tolerance to pancreatic islets is initiated in the graft and sustained in the spleen. *Am. J. Transplant.* 13: 1963–1975.
54. Fecteau, S., G. P. Basadonna, A. Freitas, C. Ariyan, M. H. Sayegh, and D. M. Rothstein. 2001. CTLA-4 up-regulation plays a role in tolerance mediated by CD45. *Nat. Immunol.* 2: 58–63.
55. Chen, G., P. P. Luke, H. Yang, L. Visser, H. Sun, B. Garcia, H. Qian, Y. Xiang, X. Huang, W. Liu, et al. 2007. Anti-CD45RB monoclonal antibody prolongs renal allograft survival in cynomolgus monkeys. *Am. J. Transplant.* 7: 27–37.
56. Yang, H., J. Arp, Y. Ma, I. Welch, A. Haig, W. Liu, K. Reimann, A. Jevnikar, and D. Rothstein. 2014. Combination of novel anti-CD45RB and anti-CD40 chimeric antibodies promotes operational tolerance and induction of T regulatory cells in cynomolgus monkey renal allograft recipients. In *World Transplant Congress*, San Francisco, CA.
57. Luke, P. P., J. P. Deng, C. A. O'Brien, M. Everest, A. V. Hall, S. Chakrabarti, P. J. O'Connell, R. Zhong, and A. M. Jevnikar. 2003. Alteration in CD45RB^{hi}/CD45RB^{lo} T-cell ratio following CD45RB monoclonal-antibody therapy occurs by selective deletion of CD45RB^{hi} effector cells. *Transplantation* 76: 400–409.